PROCEEDINGS OF SCIENCE

Complementary test of lepton flavor universality violation in $B_s \to f_2'(1525)\,(\to K^+K^-)\,\mu^+\mu^-$ decays

N Rajeev,[a,*] **Rupak Dutta**[a] **and Niladribihari Sahoo**[b]

[a] *National Institute of Technology Silchar, Silchar 788010, India*

[b] *Department of Physics, University of Warwick, Coventry CV4 7AL, United Kingdom*

E-mail: rajeev_rs@phy.nits.ac.in, rupak@phy.nits.ac.in, niladri.sahoo@warwick.ac.uk

The lepton flavor universality violation has been reported in the various flavor ratios such as R_K, R_{K^*}, and P_5' in $B \to K^{(*)}\,\mu^+\mu^-$ decays. In this context, we perform an angular analysis of the four-body differential decay of $B_s \to f_2'(1525)\,(\to K^+K^-)\,\mu^+\mu^-$ in a model independent effective field theory formalism and provide a complementary information on the lepton flavor universality violation. The underlying decay mode proceed via similar $b \to s\,l^+\,l^-$ quark level transition. We give predictions of various physical observables for $B_s \to f_2'(1525)\,(\to K^+K^-)\,\mu^+\mu^-$ decays in SM and in the presence of various NP scenarios. This can be easily tested in the ongoing LHCb experiment.

40th International Conference on High Energy physics - ICHEP2020
July 28 - August 6, 2020
Prague, Czech Republic (virtual meeting)

*Speaker

PoS(ICHEP2020)414

1. Introduction

Over the period of time, the tension in the theoretical predictions and the experimental measurements of the lepton flavor universal ratios $R_{K^{(*)}}$ and $R_{D^{(*)}}$ is reduced to some extent but the curiosity to discern the absolute understanding of the anomalies in B system remains as it is. To date, several experimental measurements in the semileptonic decays of B mesons involving $b \to s\, l^+\, l^-$ ($l \in e, \mu$) neutral current and $b \to c\, l\, \nu$ ($l \in e/\mu, \tau$) charged current quark level transitions from various B factories manifest a clear disagreement with the SM expectations which clearly hint for the lepton flavor universality violation (LFUV). In Table 1, we report the current status of R_K, R_{K^*}, P_5' in $B \to K^{(*)}\, l^+\, l^-$ decays and the branching ratio of $\mathcal{B}(B_s \to \phi\, \mu^+\, \mu^-)$.

	q^2 bins	Theoretical predictions	Experimental measurements	Deviation
R_K	[1.0, 6.0]	1 ± 0.01 [2, 3]	$0.846^{+0.060}_{-0.054}$ (stat) $^{+0.016}_{-0.014}$ (syst) [1]	$\sim 2.5\sigma$
R_{K^*}	[0.045, 1.1]	1 ± 0.01 [2, 3] 1 ± 0.01 [2, 3]	$0.660^{+0.110}_{-0.070}$ (stat) ± 0.024 (syst) [4] $0.52^{+0.36}_{-0.26}$ (stat) ± 0.05 (syst) [5]	$\sim 2.4\sigma$
	[1.1, 6.0]	1 ± 0.01 [2, 3] 1 ± 0.01 [2, 3]	$0.685^{+0.113}_{-0.069}$ (stat) ± 0.047 (syst) [4] $0.96^{+0.45}_{-0.29}$ (stat) ± 0.11 (syst) [5]	
P_5'	[4.0, 6.0]	-0.757 ± 0.074 [7]	-0.21 ± 0.15 [8–10]	$\sim 3.3\sigma$
	[4.3, 6.0]	$-0.774^{+0.0.061+0.087}_{-0.059-0.093}$ [6]	$-0.96^{+0.22}_{-0.21}$ (stat) ± 0.16 (syst) [12]	$\sim 1.0\sigma$
	[4.0, 8.0]	-0.881 ± 0.082 [14]	$-0.267^{+0.275}_{-0.269}$ (stat) ± 0.049 (syst) [13]	$\sim 2.1\sigma$
$\mathcal{B}(B_s^\phi)$	[1.0, 6.0]	$(5.39 \pm 0.66) \times 10^{-8}$ [15, 16]	$(2.57 \pm 0.37) \times 10^{-8}$ [11, 17]	$\sim 3.7\sigma$

Table 1: Current status of R_K and R_{K^*} and P_5' in $B \to K^{(*)}\, l^+\, l^-$ and the branching ratio of $\mathcal{B}(B_s \to \phi\, \mu^+\, \mu^-)$

In this context, in the present article we discuss the four body decay of $B_s \to f_2'(1525)(\to K^+K^-)\mu^+\mu^-$ which undergo similar $b \to s\, l^+\, l^-$ quark level transitions. The study of this decay mode is important because it provides complementary information regarding the LFUV in $b \to s\, l^+\, l^-$ transitions. We give predictions of various physical observables such as the branching ratio, the longitudinal polarization fraction, the forward-backward asymmetry, the angular observables P_1, P_2, P_4', P_5' and also the lepton flavor sensitive observables such as the ratio of branching ratio $R_{f_2'}$, Q_{F_L}, $Q_{A_{FB}}$, Q_1, Q_2, Q_4', Q_5' for the $B_s \to f_2'\,(1525)\,(\to K^+\,K^-)\,\mu^+\,\mu^-$ decay mode in the standard model and in the presence of several 1D and 2D new physics scenarios.

2. Model independent framework

The relevant effective Hamiltonian for $b \to s\, l^+\, l^-$ quark level transition decays in the presence of new vector and axial vector NP operators is as follows,

$$\begin{aligned}\mathcal{H}_{eff} \;=\; -\frac{G_F}{\sqrt{2}}\, V_{tb}\, V_{ts}^*\, \frac{\alpha_e}{4\,\pi}\Bigg[& C_9^{eff}\; \bar{s}\,\gamma^\mu\, P_L\, b\, \bar{l}\,\gamma_\mu\, l \;+\; C_{10}^{eff}\; \bar{s}\,\gamma^\mu\, P_L\, b\, \bar{l}\,\gamma_\mu\,\gamma_5\, l \;-\; \frac{2\,m_b}{q^2} C_7^{eff}\; \bar{s}\, i\, q_\nu \\ & \sigma^{\mu\nu}\, P_R\, b\, \bar{l}\,\gamma_\mu\, l \;+\; C_9^{NP}\; \bar{s}\,\gamma^\mu\, P_L\, b\, \bar{l}\,\gamma_\mu\, l \;+\; C_{10}^{NP}\; \bar{s}\,\gamma^\mu\, P_L\, b\, \bar{l}\,\gamma_\mu\,\gamma_5\, l \;+\; C_9'\; \bar{s}\,\gamma^\mu\, P_R\, b\, \bar{l}\,\gamma_\mu\, l \\ & + C_{10}'\; \bar{s}\,\gamma^\mu\, P_R\, b\, \bar{l}\,\gamma_\mu\,\gamma_5\, l \Bigg], \end{aligned} \tag{1}$$

where all the constants have their usual meanings as defined in [18]. Here the $C_{9,10}^{NP}$ and $C'_{9,10}$ refer to the new Wilson coefficients (WCs) which include the effects coming from the new vector-axial vector NP couplings. The factorizable loop terms are incorporated within the effective WCs C_7^{eff} and C_9^{eff} as defined in Ref. [19]. The values of each new WCs are taken from the global fit results of Ref. [20]. Using the helicity formalism we get the differential decay width and also we define various physical observables for $B_s \to f_2'(1525)\, l^+ l^-$ decays. The relevant formulas and all the omitted details can be found in Ref. [18]. Moreover, for the form factor input parameters we refer to the values evaluated in the pQCD approach as reported in [21].

3. Results and Discussions

3.1 Standard model predictions

In the SM, we obtain the branching ratio of $B_s \to f_2'(1525)(\to K^+K^-)\,\mu^+\mu^-$ decays to be of the order of $O(10^{-7})$. We obtain the similar behaviour for both e mode and μ mode of $B_s \to f_2'(1525)\, l^+ l^-$ decays. In SM as there is LFU, the observable $R_{f_2'}$ is found to be almost equal to 1 and $Q_i^{(\prime)}$ to be equal to 0. We see that the $A_{FB}(q^2)$ and $P_2(q^2)$ have zero crossing points at $q^2 \sim 3$ GeV^2. Similarly, the $P_4'(q^2)$ and $P_5'(q^2)$ have the zero crossings at $q^2 \sim 1.4$ GeV^2 and $q^2 \sim 1.6$ GeV^2. These zero crossings later help us to distinguish among various NP scenarios. The angular observable $P_1(q^2)$ is quite interesting as it is almost zero in the low q^2. The ratio of branching ratio $R_{f_2'}(q^2)$ is constant and equal to ~ 1. Interestingly, the uncertainty in $R_{f_2'}(q^2)$ is almost negligible. For all the omitted details one can refer to [18].

3.2 New physics predictions

In the effective Hamiltonian the NP can enter through several NP Lorentz structures such as vector, axial vector, scalar, pseudoscalar and tensor operators. In our analysis we do not consider the NP effects coming from the scalar, pseudoscalar and tensor NP Lorentz structures. Among the various available global fits to the $b \to s\, l^+ l^-$ data, we mainly follow the Ref. [20] for the values of new WCs. In particular, we consider $C_{9,10}^{NP}$ and $C'_{9,10}$ NP operators and they are studied in four $1D$ and three $2D$ NP scenarios. The observations are as follows.

3.2.1 1D scenario

In this section we look for the NP effects coming from C_9^{NP}, C_{10}^{NP}, $C_9^{NP} = -C_{10}^{NP}$ and $C_9^{NP} = -C_9'$ WCs. We give predictions of several observales in different q^2 bins. In the Fig. 1, we display the binned plots for $R_{f_2'}$, P_5' and Q_5'. The ratio of branching ratios $R_{f_2'}$ is significant at more than 5σ from the SM. The P_5' is little interesting in the $q^2 \in [0.045, 0.98]$ bin where the $C_9^{NP} = -C_9'$ deviate at around 1σ from the SM prediction. The Q_5' obtained in case of C_9^{NP}, $C_9^{NP} = -C_{10}^{NP}$ and $C_9^{NP} = -C_9'$ NP scenarios are clearly distinguishable from the SM prediction at more than 5σ significance. Similarly, we notice that there are deviations from the SM expectations in the branching ratio, F_L and A_{FB} due to C_9^{NP} and $C_9^{NP} = -C_{10}^{NP}$, but the $C_9^{NP} = -C_9'$ NP coupling is found to be more significant from the rest. In the case of angular observables $\langle P_1 \rangle$, $\langle P_2 \rangle$, $\langle P_4' \rangle$, $\langle P_5' \rangle$, although the SM differ slightly with respect to the different NP scenarios, no distinguishable observations are made. On the other hand, the deviations in the LFU sensitive observables are quite

interesting. In the observable Q_1, the $C_9^{NP} = -C_9'$ deviate at 5σ from the SM. Similarly, in Q_2 and Q_4' the C_9^{NP} and $C_9^{NP} = -C_9'$ NP scenarios are distinguishable from the SM prediction at more than 5σ in the particular q^2 bins. Also the $Q_{A_{FB}}$ and Q_{F_L} are distinguishable from the SM at the level of 3σ significance.

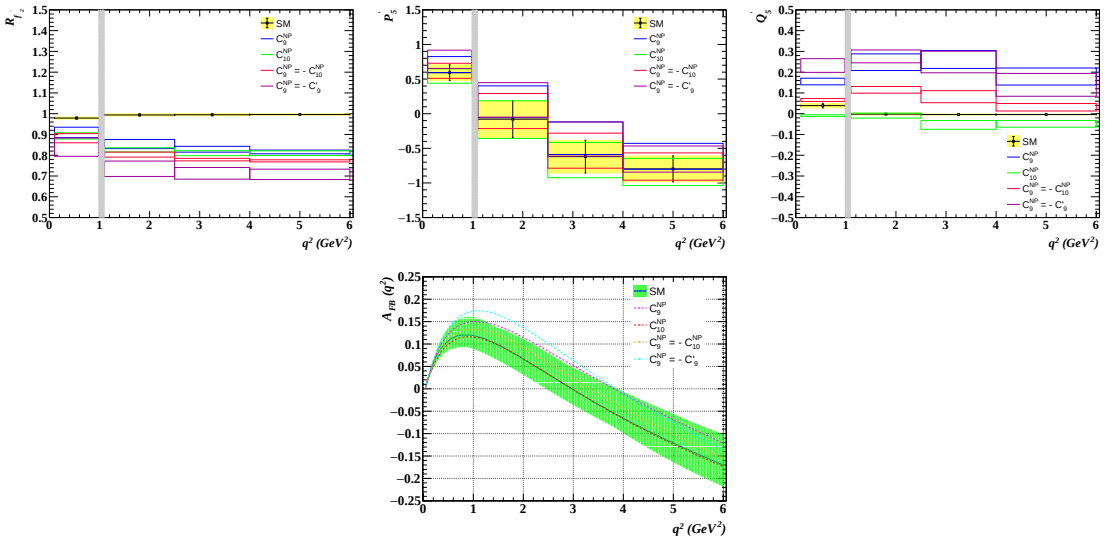

Figure 1: The binned plots of $R_{f_2'}$, P_5' and Q_5' in the top panel and the q^2 dependency of forward-backward asymmetry $A_{FB}(q^2)$ in the bottom panel in presence of 1D scenario for the $B_s \to f_2'(1525)(\to K^+K^-)\mu^+\mu^-$.

Similarly, in bottom of the Fig. 1 we show the q^2 dependency of the forward-backward asymmetry $A_{FB}(q^2)$ in which the green band is for SM and the respective colors represent various 1D NP scenarios. The $A_{FB}(q^2)$ seems to be very interesting observable since we see the zero of $A_{FB}(q^2)$ shifts towards the higher q^2 region for most of the NP scenarios as compared to the SM. However, the zero crossings for SM and C_{10}^{NP} overlaps at $q^2 \sim 3^{+0.8}_{-0.6}\,\text{GeV}^2$. Similarly, we have the zero crossing for $C_9^{NP} = -C_{10}^{NP}$ at $q^2 \sim 3.3\,\text{GeV}^2$. The zero crossings for C_9^{NP} and $C_9^{NP} = -C_9'$ NP scenarios are found at $q^2 \sim 3.8\,\text{GeV}^2$ which is distinguishable from the SM prediction at the level of 1σ significance. On the other hand, there are quite interesting observations even with the other observables such as $F_L(q^2)$, $P_2(q^2)$, $P_4'(q^2)$ and $P_5'(q^2)$. In general, the C_9^{NP} and $C_9^{NP} = -C_9'$ NP scenarios make distinguishable impact on most of the observables as compared to the SM and rest of the NP couplings. One can refer to [18] for all the omitted details.

3.2.2 2D scenario

In this section we will discuss the impact of 2D NP couplings such as (C_9^{NP}, C_{10}^{NP}), (C_9^{NP}, C_9') and (C_9^{NP}, C_{10}'). We show in the Fig. 2 the binned plots for $R_{f_2'}$, P_5' and Q_5' in the presence of 2D NP couplings. In the case of $R_{f_2'}$, all the NP scenarios are distinguishable at more than 3σ from the SM prediction and in particular, the (C_9^{NP}, C_9') and (C_9^{NP}, C_{10}') NP scenarios are quite significant at more than 5σ significance. The value of P_5' obtained in the bin $q^2 \in [0.045, 0.98]$ in case of (C_9^{NP}, C_9') NP scenario shows deviation of around 1σ from the SM prediction, whereas, with other NP scenarios, it is consistent with the SM prediction. Similarly, the Q_5' obtained in

each NP scenarios is clearly distinguishable from the SM prediction at more than 5σ significance. Interestingly, the (C_9^{NP}, C_9') NP scenario is more pronounced in most of the observables. However on the other hand, the branching ratio, F_L, A_{FB} and the angular observables $\langle P_1 \rangle$, $\langle P_2 \rangle$, $\langle P_4' \rangle$ are significant at the level of 1σ from the SM. In addition to this, the other LFU sensitive observables such as $\langle Q_{F_L} \rangle$, $\langle Q_{A_{FB}} \rangle$, and $\langle Q_i^{(\prime)} \rangle$ show very clear distinction between the SM and various NP scenarios.

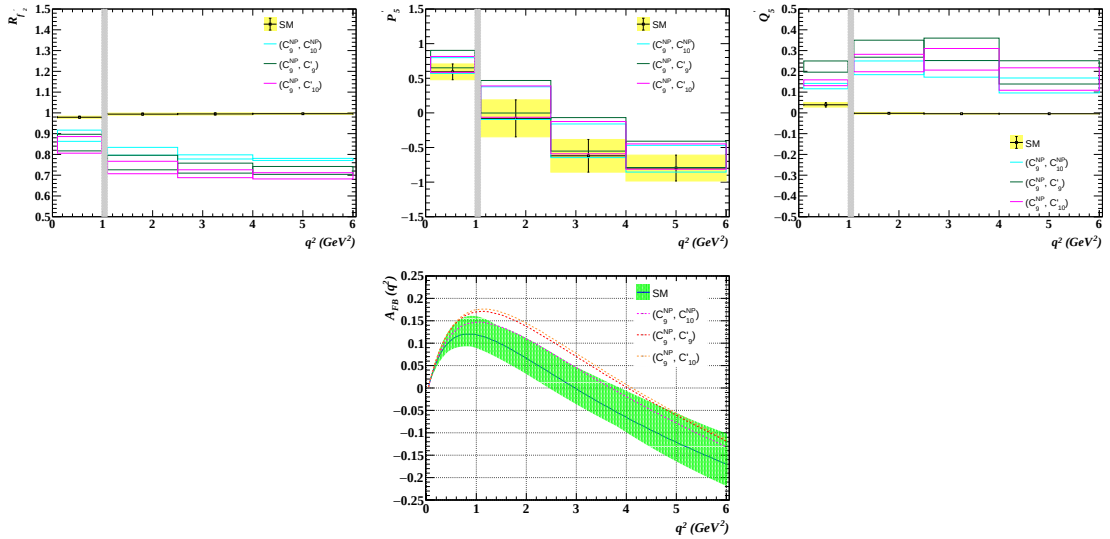

Figure 2: The binned plots of $R_{f_2'}$, P_5' and Q_5' in the top panel and the q^2 dependency of forward-backward asymmetry $A_{FB}(q^2)$ in the bottom panel in presence of 2D scenario for the $B_s \to f_2'(1525)(\to K^+K^-)\mu^+\mu^-$.

Similarly, it is worth to discuss the impact of the 2D NP couplings in the q^2 dependent observables. In the bottom of Fig. 2 we show the plot for $A_{FB}(q^2)$. As we can see the $A_{FB}(q^2)$ is shifted to higher q^2 region for all the NP scenarios as compared to the SM. The zero crossing points for $A_{FB}(q^2)$ in the case of (C_9^{NP}, C_{10}^{NP}), (C_9^{NP}, C_9') and (C_9^{NP}, C_{10}') NP scenarios respectively found at at $q^2 \sim 3.6\,\text{GeV}^2$, $q^2 \sim 4\,\text{GeV}^2$ and $q^2 \sim 4.1\,\text{GeV}^2$. In fact, the (C_9^{NP}, C_9') and (C_9^{NP}, C_{10}') NP scenarios are distinguishable at more than 1σ from the SM. Also all these values which are found in this 2D scenario are distinct from the SM as well as the 1D scenario. In addition, various other observables exhibit interesting features. The details can be found in [18].

4. Conclusion

We have performed a detailed angular study of the four body decay of $B_s \to f_2'(1525)(\to K^+K^-)\mu^+\mu^-$ in a model independent effective field theory formalism. We have given the predictions of several observables in SM and in the presence of various 1D and 2D NP scenarios. The zero crossing for $A_{FB}(q^2)$ is quite significant since it can, in principle, give useful information regarding lepton flavor universality violation in $b \to s\,l^+\,l^-$ transition decays. Interestingly, the lepton flavor sensitive observables such as $R_{f_2'}$ and Q observables are exceptionally clean with 1% of their theoretical uncertainty. In fact these observables make the ideal candidates to probe

NP in $b \to s\, l^+\, l^-$ transition decays. Comprehensively, in our NP analysis we do observe significant contributions coming from the primed WCs such as $C_9^{NP} = -C_9'$ in the 1D scenario and (C_9^{NP}, C_9') and (C_9^{NP}, C_{10}') in the 2D scenario. To this end, the theoretical understanding of the $B_s \to f_2'(1525)\, l^+\, l^-$ transition decays are crucial as they make a complementary information regarding the lepton flavor universality violation in $b \to s\, l^+\, l^-$ decays.

References

[1] R. Aaij *et al.* [LHCb], Phys. Rev. Lett. **122**, no.19, 191801 (2019)

[2] G. Hiller and F. Kruger, Phys. Rev. D **69**, 074020 (2004)

[3] M. Bordone, G. Isidori and A. Pattori, Eur. Phys. J. C **76**, no.8, 440 (2016)

[4] R. Aaij *et al.* [LHCb], JHEP **08**, 055 (2017)

[5] A. Abdesselam *et al.* [Belle], [arXiv:1904.02440 [hep-ex]].

[6] S. Descotes-Genon, J. Matias, M. Ramon and J. Virto, JHEP **01**, 048 (2013)

[7] S. Descotes-Genon, T. Hurth, J. Matias and J. Virto, JHEP **05**, 137 (2013)

[8] M. Aaboud *et al.* [ATLAS], JHEP **10**, 047 (2018)

[9] R. Aaij *et al.* [LHCb], Phys. Rev. Lett. **111**, 191801 (2013)

[10] R. Aaij *et al.* [LHCb], JHEP **02**, 104 (2016)

[11] J. Aebischer, J. Kumar, P. Stangl and D. M. Straub, Eur. Phys. J. C **79**, no.6, 509 (2019)

[12] CMS Collaboration, [CMS-PAS-BPH-15-008].

[13] A. Abdesselam *et al.* [Belle], [arXiv:1604.04042 [hep-ex]].

[14] S. Descotes-Genon, L. Hofer, J. Matias and J. Virto, JHEP **12**, 125 (2014)

[15] R. Aaij *et al.* [LHCb], JHEP **07**, 084 (2013)

[16] R. Aaij *et al.* [LHCb], JHEP **09**, 179 (2015)

[17] A. Bharucha, D. M. Straub and R. Zwicky, JHEP **08**, 098 (2016)

[18] N. Rajeev, N. Sahoo and R. Dutta, [arXiv:2009.06213 [hep-ph]].

[19] A. J. Buras and M. Munz, Phys. Rev. D **52**, 186-195 (1995)

[20] A. K. Alok, A. Dighe, S. Gangal and D. Kumar, JHEP **06**, 089 (2019)

[21] W. Wang, Phys. Rev. D **83**, 014008 (2011)